

# Lane Detection by Dynamic Origin Technique for Advanced Driver Assistance System

P.Maya, and C.Tharini

**Abstract**—Lane detection is one of the key steps for developing driver assistance and vehicle automation features. A number of techniques are available for lane detection as part of computer vision tools to perform lane detection with different levels of accuracies. In this paper a unique method has been proposed for lane detection based on dynamic origin (DOT). This method provides better flexibility to adjust the outcome as per the specific needs of the intended application compared to other techniques. As the method offers better degree of control during the lane detection process, it can be adapted to detect lanes in varied situations like poor lighting or low quality road markings. Moreover, the Piecewise Linear Stretching Function (PLSF) has also been incorporated into the proposed method to improve the contrast of the input image source. Adding the PLSF method to the proposed lane detection technique, has significantly improved the accuracy of lane detection when compared to hough transform method from 87.88% to 98.25% in day light situations and from 94.15% to 97% in low light situations.

**Keywords**—Advanced Driver Assistance System (ADAS), Machine Vision Research, Lane Detection, Piecewise Linear Stretching Function, Slope Detection

## I. INTRODUCTION

UNINTENDED lane departure can occur due to driver's inattention, poor visibility and poor road conditions and may lead to accidents & fatalities.

A driver assistance system is an automobile sub system that provides aid and assistance to the driver while driving a vehicle. This system operates by taking inputs from a multitude of sensors attached to the vehicle, processing the inputs and providing feedback to the driver in the form of notifications, alerts, warnings or based on the capabilities of the system, even actively interfering with the driver actions. The Lane Departure Warning (LDW), Adaptive Cruise Control (ACC) and Blind spot monitoring (BSM) are examples of driver assistance systems [2].

One common but vital input to all driver assistance systems is the detection of lane markings. Lane markings are an important aspect of road safety and staying within the intended lane ensures safe driving.

The standard workflow for lane detection is video ROI selection, pre-processing, edge detection, lane detection followed by driver assistance processing.

The camera in a moving vehicle capture the video from front side. The whole image has the details of road and other details like trees, name boards, sky etc. All details in the images are not required for lane detection processing. Processing the whole image is likely to reduce performance of the lane detection, hence selection of region of interest (ROI) is standard procedure to reduce the size of the image that is used for further processing. There are a number of recommendations for ROI selection. In one case, bottom portion of the image has been considered for ROI [3], [4]. In another case, quarter of the image from the bottom has been considered [6]. In yet another case ROI has been determined as the image below the vanishing point [7]. It has been further explained that when a camera is mounted on a vehicle in such a way that the optical axis of camera coincides with centre line of vehicle body, and the roll angle is  $\theta$ , the vanishing point of road image will appear in centre of vertical axis and the part of the road image that lies below the vanishing point will form the ROI. In another recommendation, 40% of image from bottom has been considered as ROI [1]. Another proposal has introduced an intelligent trapezoidal ROI [8]. The ROI selection, line detection procedure has been applied independently on the first frame and carried forward to the succeeding video frames [11].

The major problem in vision-based lane detection is handling complex situations in the given image such as poor lighting conditions, low light, rain, fog, reflections, oncoming vehicle headlights, different colours of lane markings having different interpretations and quality of lane markings. The camera is mounted on the vehicle to capture videos of the road in the front. Road conditions make the camera unstable, which adds noise in the video. Researchers have suggested different pre-processing techniques to improve the quality of input for lane detection by removing noise and errors due to unstable camera motion [12], [13], [14]. Gray scale conversion of the input image and gaussian low pass filter has been used to remove noise in [7], [15], [16]. Mean and median based smoothing operations has Adaptive threshold method has been used in pre-processing to handle various lighting condition in [3], [18]. Contrast enhancement techniques like piecewise filtering [20] & piecewise linear stretching function (PLSF) [1] have been applied for preprocessing.

Lane detection requires an edge detected image, where the edges are boundaries of various features in the image.

Edge detection is a major aspect of lane detection. Canny edge detection has been used in [3], [17], [22], [23], [24]. However, Canny edge detection has computation limitations. Sobel edge detection used in [4], [14], [20], [25], [27] has superior computational efficiency.

Lane detection is used to obtain a mathematical description of lane markings from the output of the edge detection step. The hough transform is a well-known technique, that can be used to detect arbitrary shapes and has robust performance and can be effectively used to extract linear features. Many adaptations of the Hough Transform have been proposed for lane detection. In one case, ROI has been divided into left and right zones and hough transform is applied separately to each zone to improve detection accuracy [1]. Adapting hough transform for different conditions has been discussed in [9], [20], [26], [28], [29]. Higher performance has been achieved in Modified hough transform [30], fast hough transform [1] and parallel hough transform [21].

This paper proposes another adaptation using Dynamic Origin Technique (DOT) for lane detection to achieve better results and reduce complexity.

## II. RESEARCH METHOD

### A. Data Description

The sample driving video referred in this paper has been taken from the CALTECH database [5] which has 526 frames of 360 x 240 pixels resolution. Two other videos considered in the paper are California road

video sequence 1 of 1280x800 resolution at 30fps and video sequence 2 of 640x320 resolution at 30fps. Apart from videos road images have also been considered as input for lane detection.

### B. Block Diagram

The block diagram in Fig.1 represents the process flow used for lane detection in this paper. The videos described in Section 2-1 form the input to the process. The video was divided into frames(images) for processing. A region of interest (ROI) was selected for better performance.

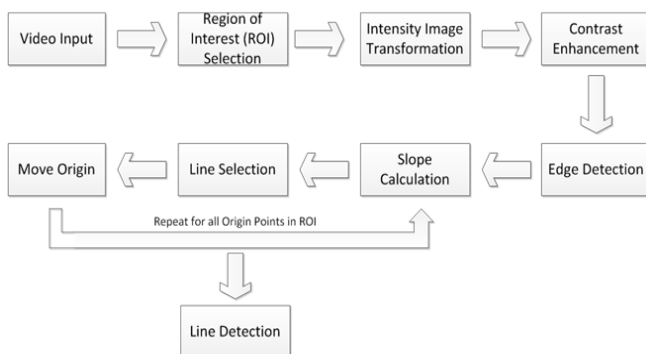


Fig. 1. Block Diagram of Proposed Lane Detection Process

The Selected ROI was converted to a gray scale image. The gray scale ROI was pre-processed with piece wise linear stretching function to improve the contrast. Sobel edge detection was performed to identify the edges of lane marking. The the Dynamic Origin technique (DOT) used to detect the lanes. Slope was calculated for all the detected edge points. Points with

similar slopes were identified and straight lines were noted. Then the origin was shifted horizontally, and the process was repeated to identify all the possible straight lines in the image.

### C. Selection of Region of Interest (ROI)

The video is segmented into frames as images. The input image is reduced in size by selecting a ROI. The video sequence from CALTECH database [5] that is referred in this paper has 526 frames of 360 x 240 resolution. ROI was selected as one third from bottom of the image. The first 4 pixels from left side, the last 4 pixels from right side and 8 pixels from bottom of the ROI are excluded. Selection of a ROI plays a major role in reducing the complexity of the lane detection. To reduce the processing time of the frame, only the selected ROI is considered for the next step. The equation number should be placed in parentheses to the right of the equation. Do not create equations as pictures. Use MathType or insert symbols as normal text.

### D. Intensity Image Transformation

Color frames from the video were transformed into intensity images. This is because, edge detection approaches taken image inputs in gray scale. In addition, gray scale images have less bits to process and there is no loss of accuracy for edge detection due to loss of colour information. RGB colour image was converted to YCbCr colour image using Eq.1. The Y component holds most of the signification information. The chrominance components Cb and Cr were ignored because these are insensitive to human visual system.

$$\begin{bmatrix} Y \\ Cb \\ Cr \end{bmatrix} = \begin{bmatrix} 0.299 & 0.587 & 0.114 \\ 0.596 & -0.275 & -0.321 \\ 0.212 & -0.523 & 0.331 \end{bmatrix} \begin{bmatrix} R \\ G \\ B \end{bmatrix} \quad (1)$$

The colour image was converted to gray image [10] and then normalized in the range [0, 1]. Lanes markings have values closer to 1 and the black and gray road surfaces have low values closer to 0. An appendix may be included (and is often helpful) in mathematical or computational modeling.

### E. Contrast Enhancement

Piecewise linear stretching method [1] was used to improve the contrast level and widen the gap between lane markings and road background. The contrast improvement is done using Eq. (2) to (6) below.

$$y = 0, 0 \leq x \leq 0.45 \quad (2)$$

$$y = 9x, 0.45 \leq x \leq 0.5 \quad (3)$$

$$y = 0.5x + 0.45, 0.5 \leq x \leq 0.6 \quad (4)$$

$$y = 3.33x + 0.5, 0.6 \leq x \leq 0.75 \quad (5)$$

$$y = 1, 0.75 \leq x \leq 1 \quad (6)$$

Fig. 7(a) shows the input color lane image. The detected edges of the binary image are shown in the Fig. 7(b). All sources cited in text must appear in the reference list, and all items in the reference list must be cited in text. With the numerical system, references are arranged in the reference list so that they match the order in which they are cited in the text.

### F. Edge Detection

The edge detection plays a major role in image processing, analyzing and recognizing features in an image. At the most basic level, edge detection involves detection the boundary

where a sharp transition from low contrast to high contrast and vice versa occurs. There are multiple edge detection algorithms available. The differential operator edge detection methods are more concise, high computational and very efficient. The differential operator edge detection method is suitable for machine vision research field and real time application. The Sobel edge operator masks are given as

$$\Delta x = \begin{bmatrix} -1 & 0 & 1 \\ -2 & 0 & 2 \\ -1 & 0 & 1 \end{bmatrix} \quad \Delta y = \begin{bmatrix} 1 & 0 & 2 \\ 0 & 0 & 0 \\ -1 & -2 & -1 \end{bmatrix} \quad (7)$$

The operator which is mentioned in Eq.7 calculates the gradient of the image intensity at each point and gives the direction of the largest possible increase from light to dark and the rate of change in that direction. This paper has used Sobel operator for edge detection.

### G. Lane Detection

Generally the hough transform is used for lane detection. Since lane detection involves processing of large streams, reducing the volume of data by using partial hough transform [31] was discussed by this author. In the paper the author proposes another technique which performs better than hough transform to perform lane detection. The proposed method set an origin and then attempted to find a line on which the maximum number of edge points above a threshold lie and pass through the origin. Then a new origin was selected incrementally, and the same exercise was repeated. Each origin will yield one line as a combination of  $(x_1, y_1, \theta)$ . Thresholds can be set to ignore lines that do not intercept a minimum number of points. In addition, once all origins were traversed, the best lines were selected as needed by applying additional criteria – for example: lane markings have to be separated by a certain distance, have to fall within certain range of slopes. Eventually, the objective was to detect the appropriate number of lines which can be considered as lanes to be provided as input into the next step.

## III. EXPLANATION OF PROPOSED TECHNIQUE - DYNAMIC ORIGIN TECHNIQUE(DOT)

The objective is to find out the slope of a line among many possible lines from an origin, which passes through the maximum number of edge points in an image.

Consider a set of detected edge points in a image with co-ordinates  $P_i(x_i, y_i)$  where  $i = 1 \dots n$ . Consider a set of origins  $O_j(x_j, y_j)$  where  $j = 1 \dots m$  from where, lines will be considered passing through the points  $P_i$ .

For a given Origin  $O(x_j, y_j)$ , calculate slope of all points  $P_i$ ,  $i = 1 \dots n$  as

$$M_i(P_i, O_j) = \frac{y_i - y_j}{x_i - x_j} \quad (8)$$

Determine the slope having the maximum frequency, that is, the slope of the line passing through the maximum number of points.

$$F_{max} = \max(\text{freq}(M_i)), \text{ where } i = 1 \dots n \quad (9)$$

$F_{max}$  represents the slope having the maximum frequency, that is, the largest number of points that have the same slope, which implies that all these points lie on a line with slope  $M_i$  passing through origin  $O_j$ .

$$M_{f_{max}} = M \text{ corresponding to } F_{max} \quad (10)$$

If  $F_{max}$  and  $M_{f_{max}}$  meet certain thresholds then  $M_{f_{max}}$  can be considered to represent a lane  $L_k$  from passing through Origin  $O_j$ .

$$L_k = T(M_{f_{max}}, O(x_j, y_j)), \text{ where } j = 1 \dots m \quad (11)$$

Repeat this process by incrementally changing the origin across the required axes. For lane detection its sufficient to incrementally change the origin across the horizontal axis of the image.

From a set of Origins  $O(x_j, y_j)$  a required number of lines which meet certain thresholds can be considered as lanes.

### H. Example for Dynamic Origin Technique (DOT)

Consider the image is shown in Figure.2, with set sample of detected edge point co-ordinates as

$$(x_i, y_i) = (6,5), (7,6), (7,16), (8,15), (9,14), (10,13), (13,11), (14,10), (15,9), (16,8) \text{ and } (17,7).$$

Compute slope of all  $N$  points using Eq.8 with respect to the first origin  $O(1, 0)$

$$M_1(P_1, O_1) = \frac{5}{6-1} = 1$$

Now repeat the process by moving the origin in the  $x$ -direction.

For Origin  $O(x_j, y_j) = (1, 0), (2,0), (3,0), (21,0), (22,0), (23,0), (24,0), (25,0)$  and  $(40,0)$ . This procedure needs to be followed till the axis is complete.

Once slopes of all points at various moved origins are computed using the Eq.(8). The Table 1 shows the slope of the given example. we need to locate the axis in which maximum numbers of similar slopes are present. The maximum numbers of similar slope calculated by the Eq.(9). This point on the axis is the location of the start point of the line.

Draw a line starting at the located point with the calculated slope. This line shall pass through the maximum number of points which can form a straight line.

Consider the points  $p_1, p_2, \dots, p_{13}$  as shown in the Fig.2.

Consider the below sample image which is the shows the plot of the detected edge points with respect to the image's left and top edges considered as the image axes. The detected edges will have a value of 1 and the rest of the image will be filled with zeroes.

The slope of each point with respect to different origins is given below.

As per Eq, 10, slopes with maximum frequency are 1.00 with frequencies of 4 and -1.00, also with a frequency of 4.00.

So the origin having maximum frequency of similar slopes is  $(12,0)$  and  $(23,0)$  and the slope of the lines at each of these origins in 1.000 and -1.000 respectively which is shown in the Table 1.

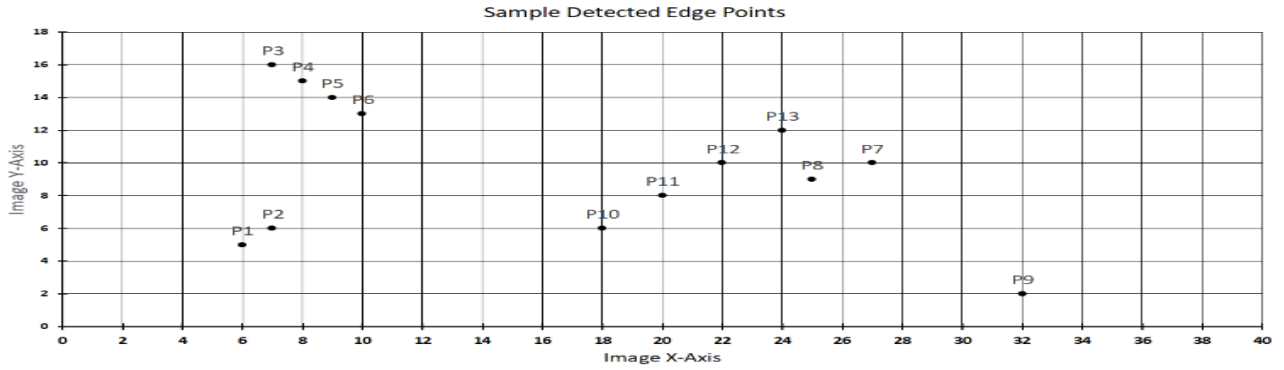


Figure 2. Sample Detected edge points

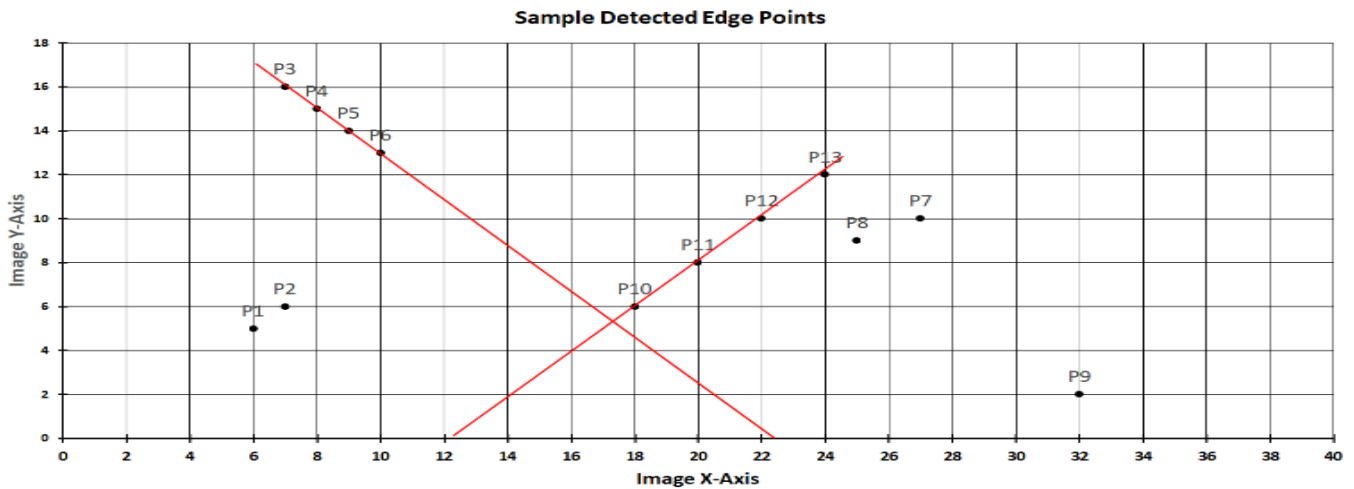


Figure 3. First set of sample detected lines for edge points

Table I  
 SLOPE OF SAMPLE DETECTED EDGE POINTS

Points	Origin→ Points(x,y)↓	(1,0)	(2,0)	(6,0)	(7,0)	(8,0)	(11,0)	(12,0)	(13,0)	(22,0)	(23,0)	(24,0)	(40,0)	
P1	(6,5)	1.000	1.250	∞	-5.000	-2.500	-1.000	-0.833	-0.714	-0.313	-0.294	-0.278	-0.147	
P2	(7,6)	1.000	1.200	6.000	∞	-6.000	-1.500	-1.200	-1.000	-0.400	-0.375	-0.353	-0.182	
P3	(7,16)	2.667	3.200	16.000	∞	-16.000	-4.000	-3.200	-2.667	-1.067	-1.000	-0.941	-0.485	
P4	(8,15)	2.143	2.500	7.500	15.000	∞	-5.000	-3.750	-3.000	-1.071	-1.000	-0.938	-0.469	
P5	(9,14)	1.750	2.000	4.667	7.000	14.000	-7.000	-4.667	-3.500	-1.077	-1.000	-0.933	-0.452	
P6	(10,13)	1.444	1.625	3.250	4.333	6.500	-13.000	-6.500	-4.333	-1.083	-1.000	-0.929	-0.433	
P7	(27,10)	0.385	0.400	0.476	0.500	0.526	0.625	0.667	0.714	2.000	2.500	3.333	-0.769	
P8	(25,9)	0.375	0.391	0.474	0.500	0.529	0.643	0.692	0.750	3.000	4.500	9.000	-0.600	
P9	(32,2)	0.065	0.067	0.077	0.080	0.083	0.095	0.100	0.105	0.200	0.222	0.250	-0.250	
P10	(18,6)	0.353	0.375	0.500	0.545	0.600	0.857	1.000	1.200	-1.500	-1.200	-1.000	-0.273	
P11	(20,8)	0.421	0.444	0.571	0.615	0.667	0.889	1.000	1.143	-4.000	-2.667	-2.000	-0.400	
P12	(22,10)	0.476	0.500	0.625	0.667	0.714	0.909	1.000	1.111	∞	-10.000	-5.000	-0.556	
P13	(24,12)	0.522	0.545	0.667	0.706	0.750	0.923	1.000	1.091	6.000	12.000	∞	-0.750	
<b>Points with same Slope</b>		2.000	2.000			4.000			4.000					
<b>Slope</b>		1.000	0.500			1.000			-1.000					

Hence as per Eq.11, the detected lines are represented by Origin – (12, 0) and slope 1.00 and Origin – (23, 0) and slope -1.00. These lines are represented in Figure. 3 below. Now drawing lines from origin as (12, 0) and (23,0) with slope -1.000 and 1.000 will pass through the maximum number of collinear points present.

**IV. RESULTS AND ANALYSIS**

The proposed novel method Dynamic Origin Technique is simulated and results are analysed. The various stages of output were shown in Figure .4 and Figure .5.

The Figure.4 shows the output from the colour video at daylight converted to frames(images).

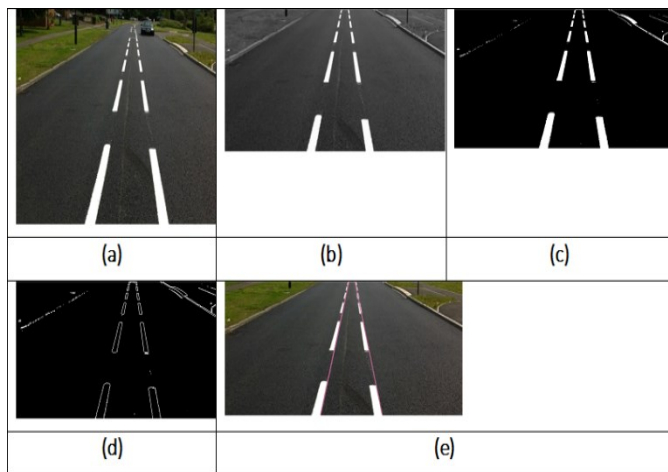


Figure 4. Experimental results of daylight image

Figure 4.(a) shows one frame from the colour video at daylight. Figure 4 (b) shows image after region of interest (ROI) selection and intensity image transformation. Figure 4(c) shows result of applying piecewise stretching function to improve contrast. Figure 4(d) shows output from Sobel edge detection. Figure 4(e) shows detected lanes by the proposed Dynamic Origin Technique (DOT)

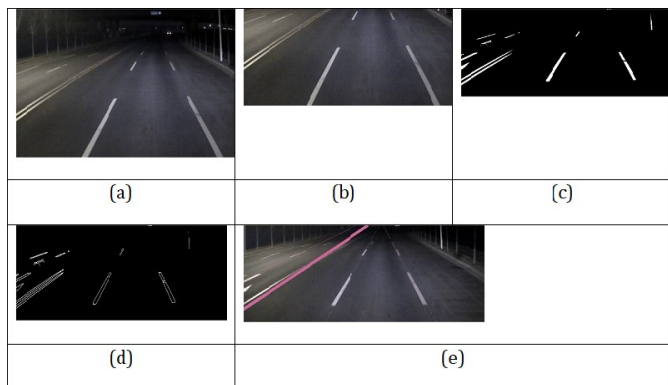


Figure 5. Experimental results of night time image

The series of image in Figure.5, are similar to the images in Figure.4 but for low light scenario. The Table. 2. and Table. 3. provides the accuracy of proposed method in lane detection. The accuracy is calculated by the Eq.12.

$$Accuracy = \left( \frac{TLDR + (1 - FLDR)}{2} \right) \times 100 \tag{12}$$

Where TLDR is True Lane Detection Rate and FLDR is False Lane Detection Rate.

TABLE II  
 ACCURACY OF THE USING DYNAMIC ORIGIN TECHNIQUE WITH VARIOUS CONDITIONS AT DAYTIME

Scenario	Type of Roads	Good Condition	Bad Condition (Fog, mist, wet etc.)
Daytime	Highway Roads	100%	97%
	City Roads	100%	96%

TABLE III  
 ACCURACY OF THE USING DYNAMIC ORIGIN TECHNIQUE WITH VARIOUS CONDITIONS AT NIGHTTIME

Scenario	Type of Roads	Good Condition	Bad Condition (Fog, mist, wet etc.)
Night time	Highway Roads	99%	98%
	City Roads	95%	96%

The Figure.6. shows that the proposed technique, has significantly improved the accuracy of lane detection when compared to other methods referred above.

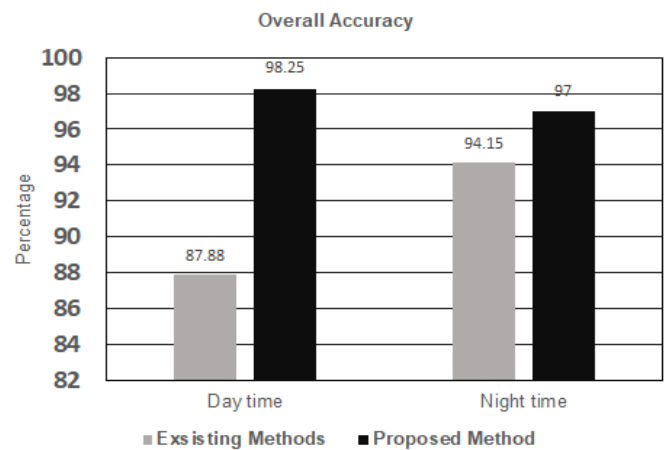


Figure 6. Accuracy Comparison

**V. CONCLUSION**

This Dynamic Origin Technique (DOT) is well suited for real-time scenarios as it offers greater degree of control over the different aspects of lane detection. The simulation results also show that this technique offers better lane detection accuracy when compared to other equivalent techniques under diverse scenarios. Further options for research could be to apply proposed method in real world scenario and observe the performance.

## REFERENCES

- [1] V. Gaikwad, S. Lokhande, "Lane departure identification for advanced driver assistance," *IEEE Transactions on Intelligent Transportation Systems*, 2015, 16(2): 910–918.
- [2] Sandipann P. Narote, Pradnya N. Bhujbal, Abhilasha S. Narote, Dhiraj M. Dhane, "A review of recent advances in lane detection and departure warning," *System. Pattern Recognition*, 2018, 73:216-234.
- [3] P.C. Wu, C. Chang, C.H. Lin, "Lane mark extraction for automobiles under complex conditions," *Pattern Recognition*, 2014, 47: 2756–2767.
- [4] C. Mu, X. Ma, "Lane detection based on object segmentation and piecewise fitting," *Telkomnika Indonesian Journal of Electrical Engineering*, 2014, 12(5):3491–3500.
- [5] CALTECH database <http://www.vision.caltech.edu/archive.html>
- [6] Y. Dong, J. Xiong, L. Li, J. Yang "Lane detection based on object segmentation and piecewise fitting," *ICCP proceedings*, 2012, 461–464.
- [7] P. Hsiao, C.W. Yeh, S. Huang, L.C. Fu, "Portable vision based real time lane departure warning system day and night," *IEEE Transactions on Vehicular Technology*, 2009, 58(4):2089–2094.
- [8] Prashanth Viswanath, Pramod Swami, "A Robust and Real-Time Image Based Lane Departure Warning System," *IEEE International Conference on Consumer Electronics*, 2016.
- [9] Minghua Niu, Jianmin Zhang, Gen Li, "Research on the Algorithms of Lane Recognition based on Machine Vision," *International Journal of Intelligent Engineering and Systems*, 2015, 8(4).
- [10] Gulivindala Suresh, Chanamallu Srinivasa Rao, "Localization of Copy-Move Forgery in Digital Images through Differential Excitation Texture Features," *International Journal of Intelligent Engineering and Systems*, 2019, 12(2).
- [11] C.R. Jung, C.R. Kelber, "Lane following and lane departure using a linear parabolic mode," *Image and Vision Computing*, 2005, 23(13):1192–1202.
- [12] D. Kragic, L. Petersson and H.I. Christensen, "Visually guided manipulation tasks," *Robotics and Autonomous Systems*, 2002, 40(2/3):193-203.
- [13] J.W. Lee, "A machine vision system for lane departure detection. Computing," *Vision Image Understanding*, 2002, 86(1): 52–78.
- [14] J. Melo, A. Naftel, A. Bernardino, J. Santos, "Detection and classification of highway lanes using vehicle motion trajectories," *IEEE Transactions on Intelligent Transportation Systems*, 2006, 7(2): 188–200.
- [15] Chaiwat Nuthong; Theekapun Charoenpong, "Lane detection using smoothing," *3rd International Congress on Image and Signal Processing*, 2010, 989-993.
- [16] Bing Yu; Weigong Zhang; Yingfeng Cai, "A Lane Departure Warning System Based on Machine Vision," *Proceeding IEEE Pacific-Asia Workshop on Computational Intelligence and Industrial Application*, 2008, 197-201.
- [17] J.G. Wang, C. Lin, S. Chen, "Applying fuzzy method to vision-based lane detection and departure warning system," *Expert Systems with Applications*, 2010, 3(1):113–126.
- [18] H. Xu, H. Li, "Study on a robust approach of lane departure warning algorithm," *IEEE International Conference on Signal Processing System (ICSPS)*, 2010, 201–204.
- [19] S. Srivastava, M. Lumb, R. Singal, "Improved Lane Detection using Hybrid Median Filter and Modified Hough Transform," *International Journal of Advanced Research in Computer Science and Software Engineering*, 2014, 4(1): 30–37.
- [20] H. Aung, M.H. Zaw, "Video based lane departure warning system using hough transform," *International Conference on Advances in Engineering and Technology (ICAET)*, 2010, 85–88.
- [21] X. An, E. Shang, J. Song, J. Li, H. He, "Real-time lane departure warning system based on a single fpga," *Eurasip Journal on Image and Video Processing*, 2013, 38(1–18).
- [22] J. Son, H. Yoo, S. Kim, K. Sohn, "Real-time illumination invariant lane detection for lane departure warning system," *Expert Systems with Applications*, 2015, 42(4):1816–1824.
- [23] Y. Wang, D. Shen, E.K. Teoh, "Lane detection using spline model," *Pattern Recognition*, 2000, 21(9): 677–689.
- [24] C.J. Lin, J.G. Wang, S.M. Chen, C.Y. Lee, "Design of a lane detection and departure warning system using functional link-based neuro-fuzzy network," *IEEE International Conference on Fuzzy System (FUZZ)*, 2010, 1–7.
- [25] Q. Lin, Y. Han, H. Hahn, "Real time lane detection based on extended edge-linking algorithm," *IEEE International Conference on Computer Research and Development*, 2010, 725–730.
- [26] C. Tu, B.V. Wyk, Y. Hamam, K. Djouni, S. Du, "Vehicle Position Monitoring using," *Hough Transform. IERI Procedia*, 2013;4:316–322.
- [27] E. Salari, D. Ouyang, "Camera-based forward collision and lane departure warning system using svm," *IEEE 56th International Midwest Symp. On Circuits and Systems (MWSCAS)*, 2013, 1278–1281.
- [28] A.S. Aguadoa, Eugenia, Montie and M. S. Nixonc, "Invariant characterisation of the Hough transform for pose estimation of arbitrary shapes," *Pattern Recognition*, 2002, 35(5):1083-1097.
- [29] Borkar, M. Hayes, M. Smith, "Robust lane detection and tracking with ransac and kalman filter," *16th IEEE International Conference on Image Processing (ICIP)*, 2009, 3261–3264.
- [30] N. Madrid, P. Hurtik "Lane departure warning for mobile devices based on a fuzzy representation of images," *Fuzzy Sets System*, 2016, 291:144–159.
- [31] P.Maya, C.Tharini, "Performance Analysis of Lane Detection Algorithm using Partial Hough Transform," *21st International Arab Conference on Information Technology (ACIT'2020)*, 2020, Egypt.